Catal Lett (2008) 124:376–383
DOI 10.1007/s10562-008-9479-4

Characterization of Cobalt Dispersed on Various Micro- and Nanoscale Silica and Zirconia Supports

Sujittra Kittiruangrayab · Tanuchnun Burakorn · Bunjerd Jongsomjit · Piyasan Praserthdam

Received: 2 March 2008 / Accepted: 18 March 2008 / Published online: 13 May 2008

Abstract Cobalt dispersion on various micro- and nanoscale SiO_2 and ZrO_2 was investigated. It revealed that Co/SiO_2 (M) exhibited higher activity than Co/SiO_2 (N) due to strong support interaction. However, Co/ZrO_2 behaved oppositely. In addition, Co dispersed on the nanoscale SiO_2 and ZrO_2 gave the similar activity for CO hydrogenation because of more uniform species.

Keywords Cobalt catalyst · Silica · Zirconia · Nanoscale · CO hydrogenation

1 Introduction

In general, a catalyst usually consists of three components: (i) a catalytic phase, (ii) a promoter, and (iii) a support or carrier. As known, the catalytic properties apparently depend upon the components as mentioned above. The catalytic phase can be metal, metal oxide, metal carbide and etc. The active form of the catalytic phase definitely depends on the specific reaction within the catalyst is applied. It is known that the performance of catalysts could be improved using a promoter such as noble metals. However, besides the consideration only in a catalytic phase and a promoter, it should be noted that a support could play a crucial role, especially as a dispersing medium for the catalytic phase. Hence, the nature of support can affect the catalytic properties based on the fact that the dispersion and interaction between a support and a catalytic phase can be altered with different supports.

For years, many inorganic supports such as SiO_2 [1–6], Al_2O_3 [7–11], TiO_2 [12–17], ZrO_2 [18], and zeolites [19] have been extensively studied. In particular, the use of mixed oxide support was also mentioned [20–22] as one of the promising ways to obtain a suitable support due to its synergetic effect arising from the mixing property. In the recent year, a significant development in nanoscience and nanotechnology has been tremendous. Therefore, many inorganic nanoscale materials have brought much attention to the research in this field [23]. However, only few studies have been done on using a nanoscale material as a support for a catalytic phase. In addition, it would be of great benefits to compare differences in characteristics between the catalytic phase dispersed on the nanoscale support and the traditional microscale support. This will lead to a significant development in a catalyst design.

In the present study, the properties of cobalt (Co) catalysts dispersed on various micro- (M) and nanoscale (N) SiO_2 and ZrO_2 supports for carbon monoxide (CO) hydrogenation reaction were investigated for comparative studies. The catalyst samples were prepared and analyzed by means of X-ray diffraction (XRD), transmission electron spectroscopy (TEM), H_2 chemisorption and temperature-programmed reduction (TPR). The reaction study was performed in order to measure activity and product selectivity toward CO hydrogenation at 220 °C and 1 atm.

2 Experimental Section

2.1 Materials

The nano-SiO_2 (10 nm) was purchased from Aldrich. The nano-ZrO_2 (35–40 nm) was prepared by flame spray

S. Kittiruangrayab · T. Burakorn · B. Jongsomjit (✉) · P. Praserthdam
Center of Excellence on Catalysis and Catalytic Reaction Engineering, Department of Chemical Engineering, Faculty of Engineering, Chulalongkorn University, Bangkok 10330, Thailand
e-mail: bunjerd.j@chula.ac.th

pyrolysis (FSP) [24]. The micro-SiO_2 was obtained from Strem chemical and the micro-ZrO_2 (ca. 0.2 microns) was purchased from Aldrich.

2.2 Preparation of Mixed SiO_2–ZrO_2 Supports

The mixed oxide support consisting of 1:1 weight ratio of ZrO_2 in SiO_2 was prepared by the solution mixing. The SiO_2 and ZrO_2 were mixed and stirred continuously in toluene (20 mL) with a magnetic stirrer for 30 min. The solvent was removed and the mixture was dried at 110 °C for 12 h and, then calcined in air at 350 °C for 2 h.

2.3 Preparation of the Supported Co Samples

A 20 wt% of cobalt dispersed on various supports was prepared by the incipient wetness impregnation. A desired amount of cobalt nitrate [$Co(NO_3)_2 \cdot 6H_2O$] (Aldrich) was dissolved in deionized water and then impregnated onto the support obtained from 2.1 and 2.2. The sample was dried at 110 °C for 12 h and calcined in air at 500 °C for 4 h.

2.4 Characterization

2.4.1 X-ray Diffraction

XRD was performed to determine the bulk crystalline phases of sample. It was conducted using a SIEMENS D-5000 X-ray diffractometer with CuK_α ($\lambda = 1.54439$ Å). The spectra were scanned at a rate of 2.4°/min in the range $2\theta = 20$–80°.

2.4.2 Transmission Electron Microscopy (TEM)

The dispersion of cobalt on various supports was determined using JEOL-TEM 200CX transmission electron spectroscopy operated at 100 kV with 50 k magnification. The sample was dispersed in ethanol prior to the TEM measurement.

2.4.3 Hydrogen Chemisorption

Static H_2 chemisorption at 100 °C on the reduced cobalt catalysts was used to determine the number of reduced surface cobalt metal atoms. This is related to the overall activity of the catalyst during CO hydrogenation. Gas volumetric chemisorption at 100 °C was performed using the method described by Reuel and Bartholomew [25]. The experiment was performed in a Micromeritics ASAP 2010 using ASAP 2010C V.3.00 software.

2.4.4 Temperature-programmed Reduction

TPR was used to determine the reduction behaviors the samples. It was carried out using 50 mg of a sample and a temperature ramp from 35 to 800 °C at 5 °C/min. The carrier gas was 5% H_2 in Ar. A cold trap was placed before the detector to remove water produced during the reaction. A thermal conductivity detector was used to determine the amount of hydrogen consumed. The hydrogen consumption was calibrated using TPR of silver oxide (Ag_2O) at the same condition.

2.5 Reaction Study

CO hydrogenation ($H_2/CO = 10/1$) was performed to measure the overall activity of the samples. Hydrogenation of CO was carried out at 220 °C and 1 atm. A flow rate of $H_2/CO/Ar = 20/2/8$ cc/min in a fixed-bed flow reactor. A relatively high H_2/CO ratio was used to minimize deactivation due to carbon deposition during reaction. Typically, 20 mg of a sample was reduced in situ in flowing H_2 (30 cc/min) at 350 °C for 10 h prior to the reaction. Reactor effluent samples were taken at 1 h intervals and analyzed by GC. In all cases, steady-state was reached within 5 h.

3 Results and Discussion

3.1 Characteristics

BET surface areas of Co catalysts on various supports are shown in Table 1. It indicated that the nanoscale supports exhibited higher surface areas than those corresponding microscale ones. XRD was performed in order to determine the bulk crystalline phases of the supports and catalysts. It can be observed that the XRD patterns for the micro- and nanoscale SiO_2 exhibited only a broad XRD peak assigning to the conventional amorphous silica. The micro- and nanoscale ZrO_2 showed the strong XRD peaks at 29 and 32 °C assigning to the ZrO_2 in the monoclinic phase. In addition, the strong XRD peaks at 30 °C, 50 °C, and 60 °C were detected for the nanoscale ZrO_2 indicating the ZrO_2 in the tetragonal phase. The XRD patterns for the mixed support of the micro- and nanoscale SiO_2–ZrO_2 only revealed the combination of SiO_2 and ZrO_2 with corresponding to their contents in the mixed supports. After impregnation of the cobalt precursor on the support, catalyst samples were dried and calcined. Besides the observation of the characteristic peaks of the supports as mentioned before, all calcined samples exhibited XRD peaks at 31 °C (weak), 36 °C (strong), and 65 °C (weak) indicating the presence of Co_3O_4. No other forms of

Table 1 Characterization results[a]

Samples	BET surface area (m_2/g)	H_2 Chemisorption		TPR	XRD
		Total (μmole H_2/g cat)	% Co dispersion[b]	Reducibility[c] 30–800 °C (%)	Co_3O_4 d_p^d (nm)
Co/SiO_2(M)	133	70	4.8	75	16
Co/SiO_2–ZrO_2(M)	57	65	4.5	68	22
Co/ZrO_2 (M)	3	28	1.9	21	66
Co/SiO_2(N)	263	55	3.8	64	n/a
Co/SiO_2–ZrO_2(N)	141	51	3.5	60	n/a
Co/ZrO_2(N)	18	47	3.2	55	n/a

[a] All the results were within ±5%

[b] Based on the total cobalt

[c] Based on the amount of H_2 consumption during TPR

[d] Determined by XRD line broadening using Scherrer's equation [26]

Co oxide species can be detected by XRD measurement. The typical XRD patterns for Co dispersed on various supports are shown in Figs. 1 and 2 for the micro- and nanoscale supports, respectively. The crystallite size of Co_3O_4 determined by XRD line broadening using Scherrer's equation [26] was shown in Table 1. However, it should be noted that the smaller crystallite size of Co_3O_4 was not the only factor to insure larger number of reduced cobalt metal surface atoms in supported Co catalysts as mentioned in our previous work [15]. Hence, implementation of other characterization techniques is crucial.

Apparently, TEM was conducted in order to identify the crystallite size and dispersion of Co oxide species on the various supports. The TEM micrographs for the various micro- and nanoscale supports are shown in Figs. 3 and 4, respectively. As seen in Fig. 3, the amorphous microscale SiO_2 exhibited only a dense of dark patches of SiO_2 whereas for the microscale ZrO_2, the crystal of ZrO_2 in the micron size (more than 100 nm in diameter) can be observed. For the mixed supports, the observation of ZrO_2 crystal was predominant. The typical TEM micrographs for various nanoscale supports are represent in Fig. 4. It can be observed that the nanoscale SiO_2 exhibited similar morphology as seen from the microscale one. However,

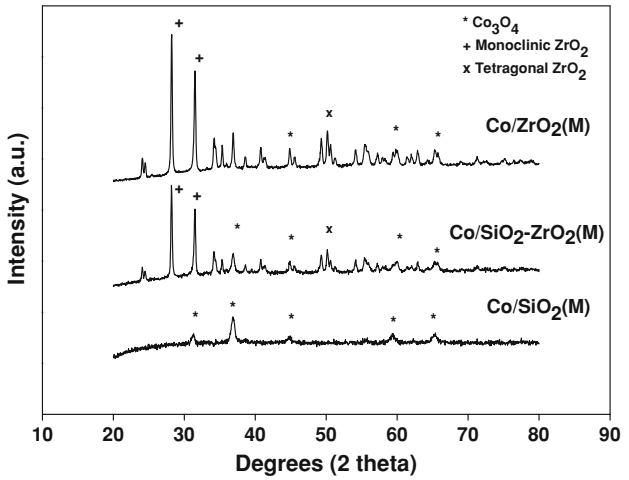

Fig. 1 XRD patterns of Co catalysts on various microscale supports

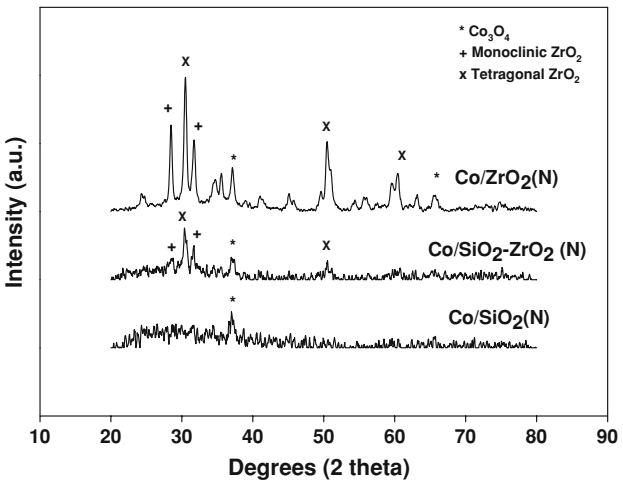

Fig. 2 XRD patterns of Co catalysts on various nanoscale supports

differences in morphologies for the micro- and nanoscale ZrO_2 were evident. Obviously, the nanoscale ZrO_2 appeared in the smaller crystal in the nano scale level (~35–40 nm). In addition, the TEM micrographs of the mixed nanoscale support also exhibited the similar appearance with those from the nanoscale ZrO_2. The dispersion of Co oxide species on the various microscale supports is shown in Fig. 5. In fact, it revealed the similar dispersion of Co for all various supports here. Although it can not differentiate the Co oxide species and ZrO_2, it indicated that Co oxide species dispersed on the microscale supports were apparently in the micron size as well. Considering the TEM micrographs for the Co oxide species dispersed on the various nanoscale supports as seen in Fig. 6, it showed very interesting results where good dispersion of Co oxide species can be achieved onto the nanoscale supports. It indicated that the dispersion of Co oxide species could be altered by the size of the support used. On the other hand, the Co oxide species dispersed on the microscale support were in the micron size whereas those were in the nano size on the nanoscale support. However, it should be noted that the highly dispersed forms of Co oxide species are not only the factor that insure large number of reduced cobalt metal surface atoms for the

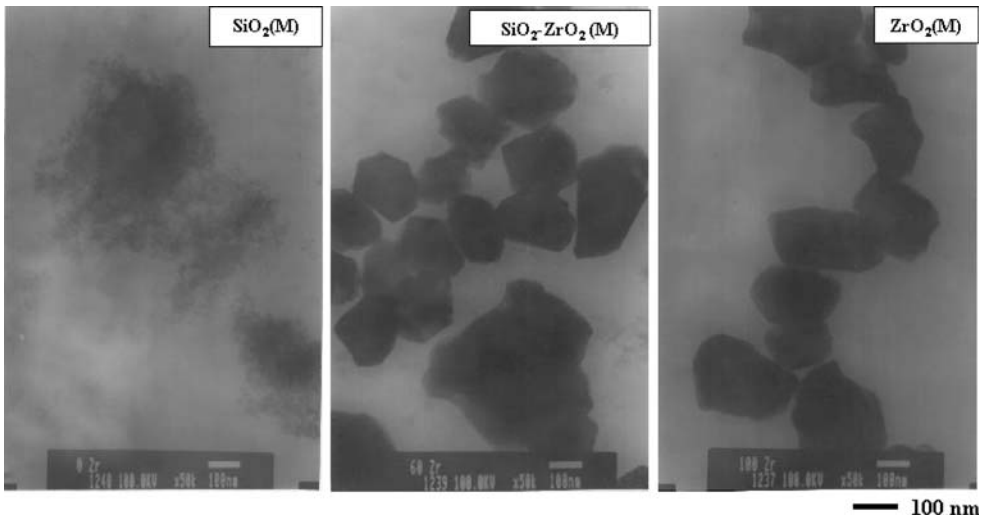

Fig. 3 TEM micrographs of various microscale supports

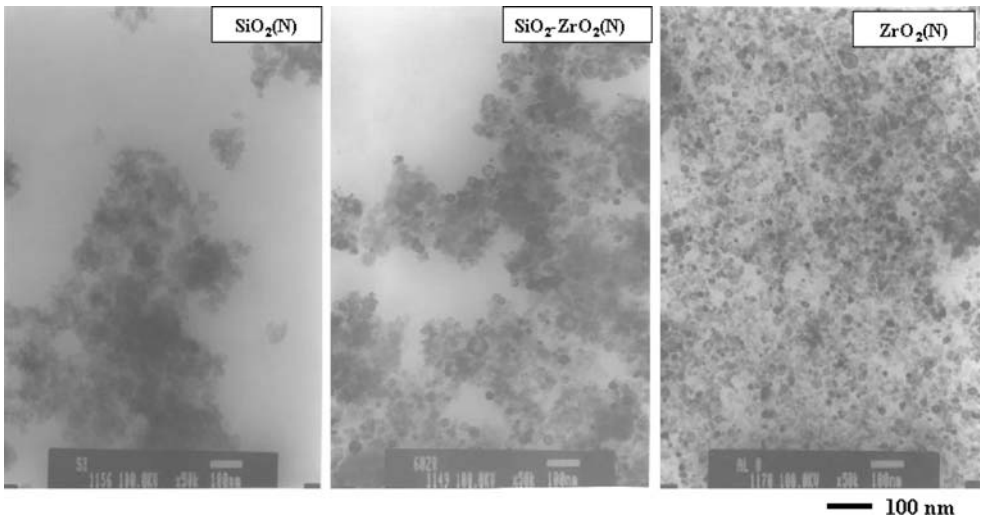

Fig. 4 TEM micrographs of various nanoscale supports

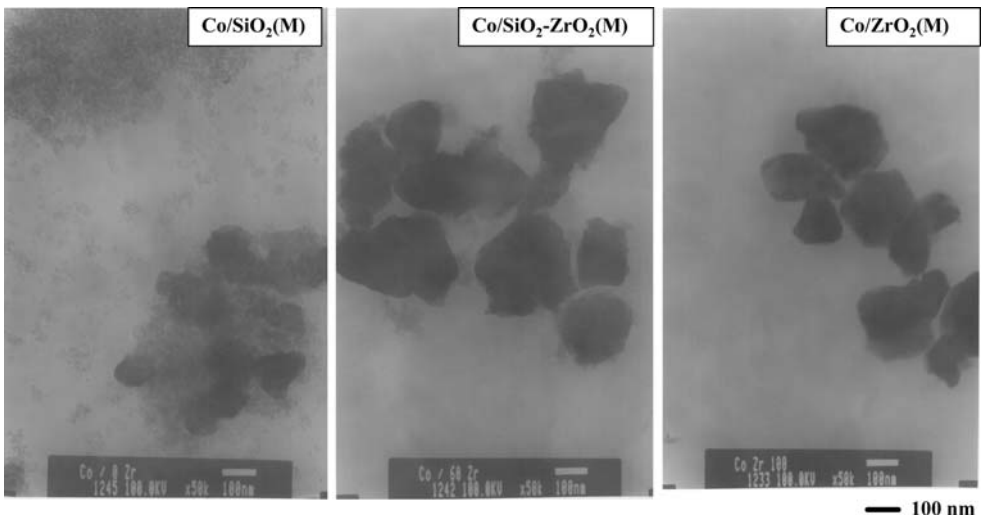

Fig. 5 TEM micrographs of Co catalysts on various microscale supports

samples as reported in our previous work [15]. Besides the dispersion of Co oxide species, the interaction between them and the support needed to be further investigated.

H_2 chemisorption results for Co on various supports are shown in Table 1. The overall dispersion of reduced Co in the catalyst samples is also given. The results indicated that

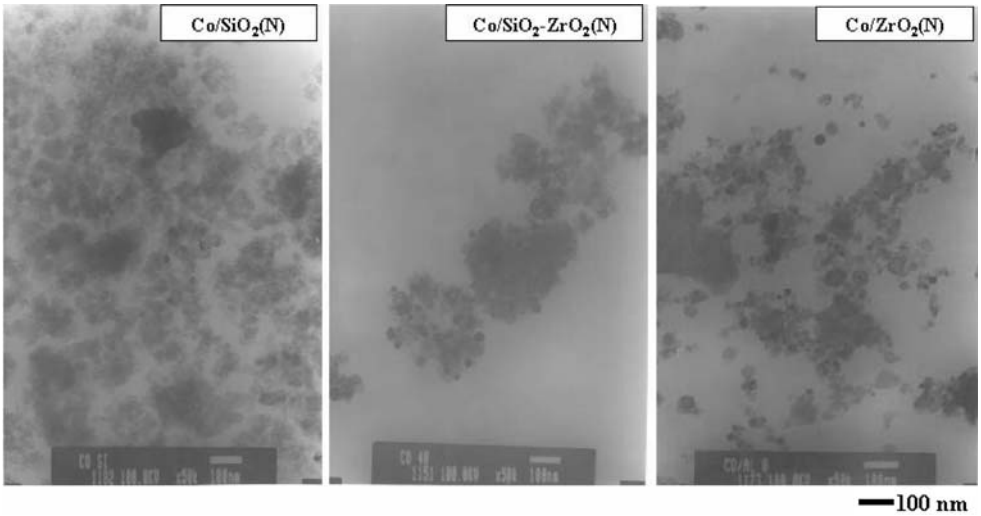

Fig. 6 TEM micrographs of Co catalysts on various nanoscale supports

the overall dispersion increased proportionally with size for SiO_2 (3.8–4.8%), but decreased with size for ZrO_2 (3.2–1.9%). The mixed micro- and nanoscale supports exhibited similar dispersion as seen for the micro- and nanoscale SiO_2, respectively. The TPR profiles of the Co catalysts on the various micro- and nanoscale supports are shown in Figs. 7 and 8, respectively. As seen in Fig. 7, Co catalysts dispersed on various microscale supports exhibited the similar TPR profiles. There were two major reduction peaks located at ca. 200 to 350 °C and 350 to 420 °C for the Co on the microscale supports. These peaks were related to the following step: Co_3O_4 to CoO, CoO to Co metal, and Co_XO_Y-support to Co metal, where Co_XO_Y-support was represented the Co oxide species strongly interacted with the support. In fact, the "strong interaction" between Co species and the support can occur during reduction and/or reaction as well. It was proposed that Co species can migrate deeply into the support. In some case, they only have the strong interaction, however, in other

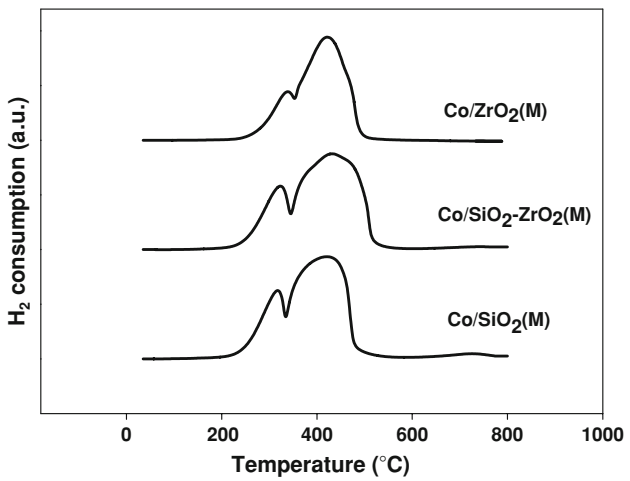

Fig. 7 TPR profiles of Co catalysts on various microscale supports

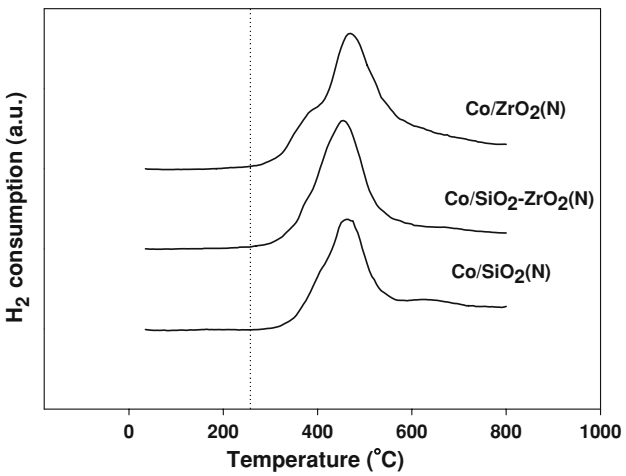

Fig. 8 TPR profiles of Co catalysts on various nanoscale supports

case, the Co-support compound formation is evident. As the results, these kinds of Co species are more difficult for reduction resulting in lower reducibility. The strong interaction apparently depends on the size of Co and nature of supports along with the reduction conditions [10]. In some cases, the peak of the decomposition of cobalt nitrates (as the precursor) during TPR of supported Co catalysts can be observed at temperatures between 200 and 300 °C, especially with silica and alumina supports [9, 10]. Prolonged calcination or reduction and recalcination resulted in completed decomposition of any cobalt nitrates present [10]. However, there was no observation of the decomposition peak of cobalt nitrate. Considering the TPR profiles of Co oxide species dispersed on the nanoscale supports as shown in Fig. 8, there was only one major reduction peak located at ca. 320 to 580 °C for the nanoscale SiO_2 and mixed SiO_2–ZrO_2 support. However, this peak was located at ca. 265 to 620 °C for the nanoscale ZrO_2. Again this peak was also related to the reduction of Co_3O_4 to CoO,

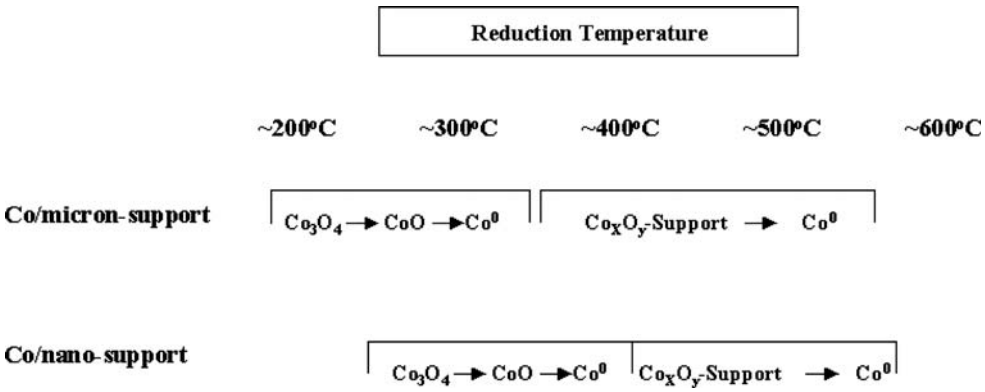

Scheme 1 Suggested reduction behaviors of Co catalysts on micro- and nanoscale supports

CoO to Co metal, and Co_XO_Y-support to Co metal as mentioned before. It should be noted that with using the nanoscale support, the interaction of Co oxide species was more homogeneous leading to only one reduction peak observed. In order to give a better understanding, the suggested reduction behaviors of Co oxide species on different micro- and nanoscale supports are shown in Scheme 1. The reducibilities during TPR from 30 to 800 °C for the catalysts are shown in Table 1. They ranged from 75 to 21% for Co on the microscale supports and from 64 to 55% for Co on the nanoscale supports. The results indicated that the reducibility of samples increased with size when SiO_2 and mixed SiO_2–ZrO_2 supports were employed. On the contrary, the reducibility of Co/ZrO_2 increased when the nanoscale ZrO_2 was used. It can be observed that the TPR results were in accordance with those obtained from H_2 chemisorption. Considering the effect of strength of metal-support interaction, the % reduction and H_2 chemisorption, which are related to the overall activity during CO hydrogenation, are altered with different strengths. It seems that the strength of metal-support interaction does not depend on the available support surface areas at this level.

3.2 Reactivity

CO hydrogenation was performed to measure the overall activity of the catalyst samples on various micro- and nanoscale supports. The reaction rate and product selectivity during CO hydrogenation at steady-state are revealed in Table 2. For the Co catalysts on SiO_2, it can be observed that the catalyst on the microscale SiO_2 exhibited higher activity than that on the nanoscale SiO_2 support without any changes in the product selectivity. However, when the SiO_2 support was mixed with ZrO_2 for both micro- and nanoscale supports, the similar trend regarding the activity and product selectivity as seen with the pure SiO_2 was still consistently observed. It was suggested that the effect of SiO_2 was more pronounced comparing with ZrO_2. Considering when ZrO_2 support was employed, the result was essentially opposite. It indicated that the catalyst on the nanoscale ZrO_2 exhibited higher activity than that on the microscale ZrO_2 support. In addition, the selectivity to C_2–C_4 was slightly higher with the ZrO_2 support. These results based on the use of ZrO_2 support were in accordance with those reported by Panpranot et al. [23]. The increased activity for the nanoscale ZrO_2 support can be attributed to the larger number of reduced Co metal surface atoms as seen from TPR and H_2 chemisorption results. Since CO hydrogenation is a structure insensitive reaction, thus, the catalytic activity depends only on the number of reduced Co metal surface atoms available for catalyzing the reaction. Considering the TOFs of samples, they are also shown in Table 2. Obviously, they are in the range of 10^{-2} s^{-1}-typical for Co catalyst under this condition [5, 9]. The calculated TOFs at steady-state based on H_2 chemisorption were found to be similar among samples [except for the Co/ZrO_2 (M)]. Since TOF is basically related to the intrinsic activity by definition, this indicates that no changes in the intrinsic activity of samples occurred. However, the low TOF of Co/ZrO_2 (M) sample was probably due to deactivation of the catalyst during time-on-stream to steady-state resulting in remarkably decreased activity during CO hydrogenation.

In particular, differences in the catalytic performance based on using the micro- and nanoscale SiO_2 and ZrO_2 supports can be described by the reduction behaviors of the catalysts on various supports. It is known that the TPR peak locations are affected by reduction kinetics. A wide range of variables including particle size, support interaction and the reduction gas composition [9] can affect the kinetics of reduction. The effects of particle size and support interaction can be superimposed on each other. Thus, while a decrease in metal oxide particle size can result in faster reduction due to a greater surface area/volume ratio, smaller particles may interact more with the support, slowing reduction. Based on the study, the particle size and nature of support could play a major role on the strength of

Table 2 Reaction rate and product selectivity during CO hydrogenation at steady-state

Sample	Reaction rate ($\times 10^2$ gCH_2/g cat h)		TOF_H^a ($\times 10^2$ S^{-1})		Product selectivity (%)			
	N	M	N	M	C_1		C_2–C_4	
					N	M	N	M
Co/SiO_2	29.9	37.5	5.4	5.3	99.5	99.2	0.5	0.8
Co/SiO_2–ZrO_2	28.0	37.3	5.4	5.7	99.1	99.6	0.9	0.4
Co/ZrO_2	25.3	5.3	5.3	1.9	96.3	95.8	3.7	4.2

[a] Based on total H_2 chemisorption

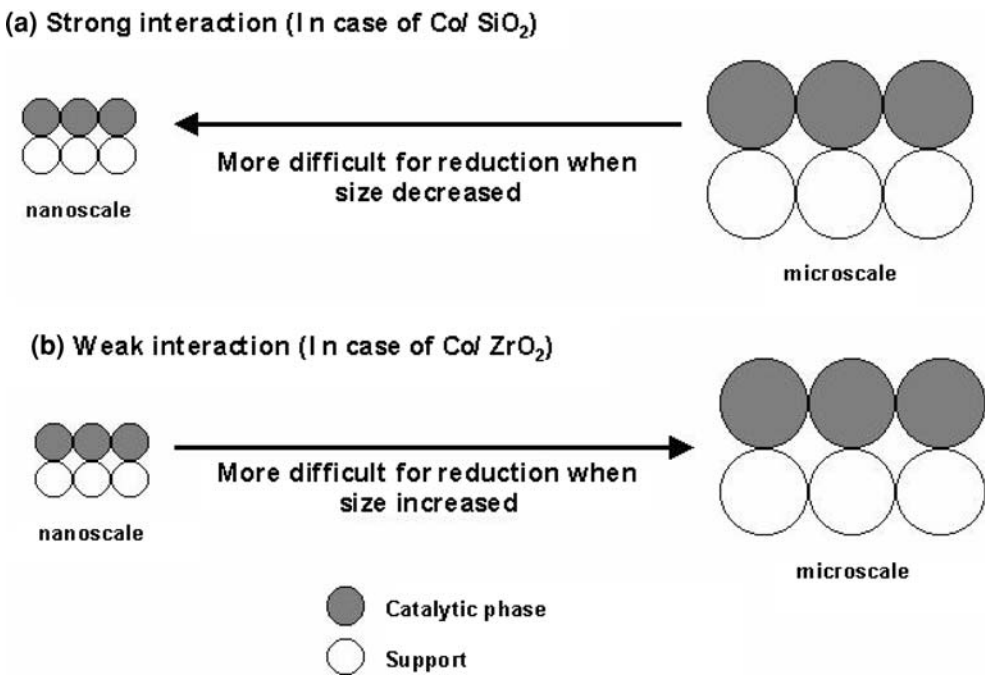

Scheme 2 Conceptual model for reduction behaviors regarding the size and nature of supports (strong and weak interaction)

metal-support interaction. Too strong interaction can result in decreased reducibility of the Co catalyst. In order to give a better understanding, a conceptual model for reduction behaviors regarding the size and nature of supports (weak or strong interaction) is shown in Scheme 2. First, it should be mentioned that the sizes of Co species dispersed on various supports were corresponding to the size of supports used (as seen by TEM). The Co/SiO_2 is considered to have a strong interaction (by nature of SiO_2) as represented by Scheme 2a. Thus, small particles (i.e. nanoscale) can interact more resulting in decreased reducibility and Co dispersion. As the results, Co/SiO_2 (N) renders lower activity than the Co/SiO_2 (M). In contrast, Co/ZrO_2 has weak interaction (by nature of ZrO_2) as represent by Scheme 2b. Due to the weak interaction, the small particles [Co/ZrO_2 (N)] are more reducible than the larger particles. Thus, the Co/ZrO_2 (N) exhibits higher activity than the Co/ZrO_2 (M).

4 Conclusions

Based on the present study, it can be concluded as follows:

1. The size of Co oxide species dispersed on a support was corresponding to the size of the support employed.
2. Besides the support interaction and particle size, the nature of supports plays important roles.
3. For the SiO_2 support, the catalyst dispersed on microscale SiO_2 was more active due to the strong interaction between SiO_2 and the catalyst. Hence, the larger particle can be reduced more easily.

4. For the ZrO_2 support, the catalyst dispersed on the nanoscale ZrO_2 was more active due to the weak interaction between ZrO_2 and the catalyst. Hence, the smaller particle can be reduced more easily.
5. Use of mixed SiO_2–ZrO_2 supports apparently resulted in similar properties with the sole SiO_2 support due to the fact that interaction of SiO_2 with Co oxides species was predominant (strong interaction).

Acknowledgment We gratefully acknowledge the financial support by the National Research Council of Thailand (NRCT), the Thailand Research Fund (TRF) and Thailand-Japan Technology Transfer Project (TJTTP-JBIC). We thank Prof. James G. Goodwin, Jr. at Clemson University for initiating the CO hydrogenation of project.

References

1. Martinez A, Lopez C, Marquez F, Diaz I (2003) J Catal 220:486
2. Panpranot J, Goodwin Jr JG, Sayari A (2002) Catal Today 77:269
3. Panpranot J, Goodwin Jr JG, Sayari A (2002) J Catal 211:530
4. Sun SL, Tsubaki N, Fujimoto K (2000) Appl Catal A 202:121
5. Jongsomjit B, Panpranot J, Goodwin Jr JG (2003) J Catal 215:66
6. Jongsomjit B, Kaewkrajang P, Wanke SE, Praserthdam P (2004) Catal Lett 94:205
7. Das T, Jacobs G, Patterson PM, Conner WA, Li JL, Davis BH (2003) Fuel 82:805
8. Jacobs G, Patterson PM, Zhang YQ, Das T, Li JL, Davis BH (2002) Appl Catal A 233:215
9. Jongsomjit B, Goodwin Jr JG (2002) Catal Today 77:191
10. Jongsomjit B, Panpranot P, Goodwin Jr JG (2001) J Catal 204:98
11. Li JL, Jacobs G, Das T, Davis BH (2002) Appl Catal A 233:255
12. Jacobs G, Das T, Zhang YQ, Li JL, Racoillet G, Davis BH (2002) Appl Catal A 233:263
13. Li JL, Xu LG, Keogh R, Davis BH (2000) Catal Lett 70:127
14. Jongsomjit B, Sakdamnuson C, Goodwin Jr JG, Praserthdam P (2004) Catal Lett 94:09
15. Jongsomjit B, Wongsalee T, Praserthdam P (2005) Mater Chem Phys 92:72
16. Jongsomjit B, Wongsalee T, Praserthdam P (2005) Catal Comm 6:705
17. Wongsalee T, Jongsomjit B, Praserthdam P (2006) Catal Lett 108:55
18. Panpranot J, Taochaiyaphum N, Praserthdam P (2005) Mater Chem Phys 94:207
19. Li XH, Asami K, Luo MF, Michiki K, Tsubaki N, Fujimoto K (2003) Catal Today 84:59
20. Jongsomjit B, Ngamposri S, Praserthdam P (2005) Catal Lett 100:139
21. Jongsomjit B, Ngamposri S, Praserthdam P (2005) Molecules 10:672
22. Jongsomjit B, Ngamposri S, Praserthdam P (2005) Ind Eng Chem Res 44:9059
23. Panpranot J, Taochaiyaphum N, Jongsomjit B, Praserthdam P (2006) Catal Comm 7:192
24. Mueller R, Jossen R, Pratsinis SE, Watson M, Akhtar MK (2004) J Am Ceram Soc 87:197
25. Reuel RC, Bartholomew CH (1984) J Catal 85:63
26. Klug HP, Alexander LE (1974) X-ray diffraction procedures for polycrystalline amorphous, 2nd edn. Wiley, New York